Analytical Approximation of Two-Dimensional Separated Turbulent Boundary-Layer Velocity Profiles

T. W. Swafford
ARO, Inc.

October 1980

Final Report for Period October 1, 1978 — April 15, 1979

ARNOLD ENGINEERING DEVELOPMENT CENTER
ARNOLD AIR FORCE STATION, TENNESSEE
AIR FORCE SYSTEMS COMMAND
UNITED STATES AIR FORCE

This report has been reviewed by the Office of Public Affairs (PA) and is releasable to the National Technical Information Service (NTIS). At NTIS, it will be available to the general public, including foreign nations.
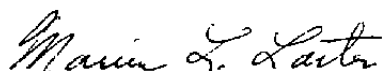
APPROVAL STATEMENT

This report has been reviewed and approved.

ELTON R. THOMPSON
Project Manager
Directorate of Technology

Approved for publication:

FOR THE COMMANDER

MARION L. LASTER
Director of Technology
Deputy for Operations

REPORT DOCUMENTATION PAGE		READ INSTRUCTIONS BEFORE COMPLETING FORM
1 REPORT NUMBER AEDC-TR-79-99	2 GOVT ACCESSION NO.	3 RECIPIENT'S CATALOG NUMBER
4 TITLE (and Subtitle) ANALYTICAL APPROXIMATION OF TWO-DIMENSIONAL SEPARATED TURBULENT BOUNDARY-LAYER VELOCITY PROFILES		5 TYPE OF REPORT & PERIOD COVERED Final Report, October 1, 1978 - April 15, 1979
		6 PERFORMING ORG REPORT NUMBER
7 AUTHOR(s) T. W. Swafford, ARO, Inc., a Sverdrup Corporation Company		8 CONTRACT OR GRANT NUMBER(s)
9 PERFORMING ORGANIZATION NAME AND ADDRESS Arnold Engineering Development Center Air Force Systems Command Arnold Air Force Station, Tennessee 37389		10 PROGRAM ELEMENT PROJECT TASK AREA & WORK UNIT NUMBERS Program Element 65807F
11 CONTROLLING OFFICE NAME AND ADDRESS Arnold Engineering Development Center/DOS Air Force Systems Command Arnold Air Force Station, Tennessee 37389		12 REPORT DATE October 1980
		13 NUMBER OF PAGES 23
14 MONITORING AGENCY NAME & ADDRESS(if different from Controlling Office)		15 SECURITY CLASS (of this report) UNCLASSIFIED
		15a DECLASSIFICATION DOWNGRADING SCHEDULE N/A

16 DISTRIBUTION STATEMENT (of this Report)

Approved for public release; distribution unlimited.

17 DISTRIBUTION STATEMENT (of the abstract entered in Block 20, if different from Report)

18 SUPPLEMENTARY NOTES

Available in the Defense Technical Information Center (DTIC).

19 KEY WORDS (Continue on reverse side if necessary and identify by block number)

turbulent boundary layer   two dimensional
velocity profile
separation
thickness
correlation techniques

20 ABSTRACT (Continue on reverse side if necessary and identify by block number)

A single analytical expression is proposed to describe the velocity distribution in a two-dimensional, separated, turbulent boundary layer on smooth, impermeable, adiabatic walls over the domain $0 \leqslant y < \infty$. The expression is an extension of one previously derived for attached flow which depends upon local values of skin friction, shape factor, and Reynolds number based on momentum thickness. Boundary-layer shape factor and local skin friction correlations applicable to separated flows are derived from fitting

DD FORM 1473 EDITION OF 1 NOV 65 IS OBSOLETE
1 JAN 73

20. ABSTRACT, (Concluded).

the proposed analytical expression for separated velocity profiles to available experimental data. These correlations are then available for analytically describing separated velocity profiles without further fitting.

AFSC
Arnold AFS Tenn

PREFACE

The work reported herein was conducted by the Arnold Engineering Development Center (AEDC), Air Force Systems Command (AFSC). The results of the research were obtained by ARO, Inc., AEDC Group (a Sverdrup Corporation Company), operating contractor for the AEDC, AFSC, Arnold Air Force Station, Tennessee, under ARO Project Number P32A-01. The Air Force project manager was Mr. Elton R. Thompson, AEDC/DOT. The data analysis was completed on April 15, 1970, and the manuscript was submitted for publication on November 27, 1979.

CONTENTS

ILLUSTRATIONS

Figure

TABLE

1.0 INTRODUCTION

The calculation of two-dimensional, turbulent, separated flow using the boundary-layer equations has achieved some degree of success, as reported in Refs. 1 through 5. Provided solutions of the boundary-layer equations yield acceptable engineering accuracy, their use to compute flows with separation is attractive because of simplicity and cost reduction compared to solution of the full Navier-Stokes equations. Boundary-layer computation methods can be classed as either integral or differential techniques. In general, integral methods are simpler and require fewer computational resources than do differential methods because of the built-in empiricism such as a velocity profile representation and auxiliary relations for shape factors, skin friction, etc. This report presents a means of analytically describing separated turbulent boundary-layer velocity profiles. The velocity profile representation is used to develop a skin friction and shape factor correlation for turbulent separated flow.

2.0 ANALYTICAL DESCRIPTION OF SEPARATED BOUNDARY-LAYER VELOCITY PROFILES

The equation proposed to describe reversed flow velocity profiles on smooth, impermeable, adiabatic walls is an extension of the expression presented by Whitfield (Ref. 6), which is a composite function of the form

$$\bar{u}^+ = \bar{u}_i^+ + \bar{u}_o^+ \tag{1}$$

which consists of an inner expression originally presented in Ref. 7 and an outer expression derived in Ref. 6. The inner solution as presented in Ref. 6 is given by

$$\bar{u}_i^+ = \frac{1}{0.09} \tan^{-1} (0.09 \, \bar{y}^+) \tag{2}$$

where

$$\bar{u}_i^+ = \frac{\bar{u}_i}{\bar{u}_\tau} \tag{3}$$

$$\bar{y}^+ = \frac{\bar{u}_\tau \bar{y}}{\nu} \tag{4}$$

5

$$\bar{u}_r = (\bar{C}_f/2)^{1/2}\,\bar{u}_e \tag{5}$$

and the subscript "i" refers to the inner region. Assumptions made in deriving Eq. (2) for attached flow were as follows: (1) the total shear stress (molecular plus turbulent) is constant and equal to the wall value, $\bar{\tau}_w$; (2) the density is constant in the wall region; (3) the turbulent kinetic energy is proportional to the Reynolds stress, $-<u'v'>$; and (4) the turbulent kinetic energy (or $-<u'v'>$) is an explicit function of $\bar{u}^+$. These assumptions are also made herein to retain the form of Eq. (2).

The slope of the velocity profile at the wall, computed from Eq. (2), is positive for $\bar{C}_f > 0$. A negative slope for separated flow can be obtained by taking the velocity distribution as

$$\bar{u}_i^+ = \frac{-1}{0.09}\,\tan^{-1}(0.09\,\bar{y}^+) \tag{6}$$

and defining $\bar{u}_r$ as

$$\bar{u}_r = \left(|\bar{C}_f|/2\right)^{1/2}\bar{u}_e \tag{7}$$

The outer expression is derived such that the complete solution, Eq. (1), approaches the correct asymptotes at the wall and infinity. From Eq. (6), as $y \to \infty$, $\bar{u}_i^+ \to -\pi/0.18$. Therefore, for $\bar{u}^+$ to have the correct limiting value of $\bar{u}_e^+$ as $y \to \infty$, $\bar{u}_0^+$ must behave as

$$\bar{u}_0^+ \to \left[\bar{u}_e^+ - \left(-\frac{\pi}{0.18}\right)\right] \tag{8}$$

as $y \to \infty$. In addition, because $\bar{u}_i^+$ behaves correctly for small values of y, $\bar{u}_0^+$ must behave as $\bar{u}_0^+ \to 0$ as $y \to 0$. Therefore, in terms of the outer variable, $\bar{y}/\bar{\theta}$, the form considered in Ref. 6,

$$\bar{u}_0^+ = \left[\bar{u}_e^+ - \left(-\frac{\pi}{0.18}\right)\right] g\left(\frac{\bar{y}}{\bar{\theta}}\right) \tag{9}$$

is retained, where $g(\bar{y}/\bar{\theta})$ behaves as $g(0) = 0$ and $g(\infty) = 1$.

In Ref. 6, the form of $g(\bar{y}/\bar{\theta})$ was determined from the analytical relation for attached flows, as follows:

$$g\left(\frac{\overline{y}}{\theta}\right) = \frac{\overline{u}^+ - \overline{u}_i^+}{\left[\overline{u}_e^+ - \frac{\pi}{0\ 18}\right]} \tag{10}$$

This relationship was plotted versus $\overline{y}/\overline{\theta}$ for numerous experimentally measured velocity profiles. The resulting curves were analytically fit by the relation

$$g\left(\frac{\overline{y}}{\theta}\right) = \tanh^{1/2}\left[a\left(\frac{\overline{y}}{\theta}\right)^b\right] \tag{11}$$

where a and b are parameters that are functions of $\overline{C}_f$, $\overline{H}$, and $\overline{Re}_\theta$. This same functional form (Eq. 11) is retained in the present work. Therefore, the analytical representation of two-dimensional, separated, turbulent boundary-layer velocity profiles becomes

$$\overline{u}^+ = \frac{-1}{0.09} \tan^{-1}(0.09\,\overline{y}^+) - \left[\overline{u}_c^+ - \left(-\frac{\pi}{0\ 18}\right)\right]\tanh^{1/2}\left[a\left(\frac{\overline{y}}{\theta}\right)^b\right] \tag{12}$$

where

$$\overline{u}_e^+ = \left(2\,/\,|\overline{C}_f|\right)^{1/2}$$

$$\overline{y}^+ = \frac{\overline{Re}_\theta}{\overline{u}_c^+} \cdot \frac{\overline{y}}{\theta}$$

$$\frac{\overline{u}}{\overline{u}_e} = \frac{\overline{u}^+}{\overline{u}_e^+}$$

The only difference between the expression derived in Ref. 6 (for attached flow) and Eq. (12) is the appearance of a negative sign in the coefficients of the trigonometric functions which is a consequence of modifying Eq. (2) so that a negative velocity slope occurs at the wall for separated flow. Thus, a convenient method to extend the result obtained in Ref. 6 for attached boundary-layer velocity profiles to include profiles with reversed flow is to define

$$S = \frac{\overline{C}_f}{|\overline{C}_f|} \tag{13}$$

and rewrite Eq. (12) as

7

$$\overline{u}^+ = \frac{S}{0.09} \tan^{-1} (0.09\,\overline{y}^+) + \left(\overline{u}_e^+ - \frac{S\pi}{0.18}\right) \tanh^{\frac{1}{2}} \left[a\left(\frac{\overline{y}}{\theta}\right)^b\right] \tag{14}$$

where the parameters a and b are functions of $\overline{C}_f$, $\overline{H}$, and $\overline{Re}_\theta$.

3.0 PROFILE CORRELATIONS

3.1 FITTING OF VELOCITY PROFILES

Experimentally measured velocity profiles were used to determine the parameters a, b, and $\overline{u}_e^+$ which appear in Eq. (14). The determination of $\overline{u}_e^+$ provides a means of estimating skin friction for separated flows in a manner similar to that used by Clauser (Ref. 8) for attached, incompressible, turbulent boundary layers. Unfortunately, only two experiments involving detailed flow measurements in a separated turbulent boundary layer could be found in the literature: the experiment of Simpson et al. (Ref. 9), which involved an incompressible flow with an airfoil-type pressure distribution, and the experimental investigation of Alber et al. (Ref. 10), who probed the transonic flow over a bump on a wind tunnel wall.

Rearranging the argument of the inverse tangent term of Eq. (14),

$$\overline{y}^+ = \frac{\overline{Re}_\theta}{\overline{u}_e^+} \cdot \frac{\overline{y}}{\theta} \tag{15}$$

yields

$$\overline{y}^+ = \left(\frac{\overline{Re}}{\overline{u}_e^+}\right)\overline{y} \tag{16}$$

where

$$\overline{u}_e^+ = \left(2/|\overline{C}_f|\right)^{\frac{1}{2}} \tag{17}$$

Also, the argument of the hyperbolic tangent function of Eq. (14) can be written as

$$a\left(\frac{\overline{y}}{\theta}\right)^b = \left(\frac{a}{\theta^b}\right)\overline{y}^b = \tilde{a}\overline{y}^b \tag{18}$$

where

$$\bar{a} = \left(\frac{a}{\bar{\theta}^{b}} \right) \qquad (19)$$

Therefore, Eq. (14) becomes

$$\bar{u}^{+} = \frac{S}{0.09} \tan^{-1} \left[0.09 \left(\frac{\overline{Re}}{\bar{u}^{+}_{e}} \right) \bar{y} \right] + \left(\bar{u}^{-}_{e} - \frac{S_{\pi}}{0.18} \right) \tanh^{1/2} \left[\bar{a} \, \bar{y}^{b} \right] \qquad (20)$$

The important consequence of the latter manipulations is that the velocity ratio $\bar{u}/\bar{u}_e$ ($\bar{u}/\bar{u}_e$ = $\bar{u}^{+}/\bar{u}^{+}_{e}$) is now a function of the physical distance, y, local unit Reynolds number, and local skin friction (incompressible). Because the available experimental data do not have significant compressibility effects, the approximation $\overline{Re} \cdot \bar{y} \approx Re \cdot y$ was used. Therefore, given $\bar{u}/\bar{u}_e$ at three points in the boundary layer, a system of three equations [Eq. (20) for each point] with three unknowns [skin friction (in terms of $\bar{u}^{-}_{e}$), $\tilde{a}$, and b] is obtained. With $\bar{u}^{+}_{e}$, $\tilde{a}$, and b known, one can obtain $\bar{\theta}$ using Eq. (20) and determine a from Eq. (19).
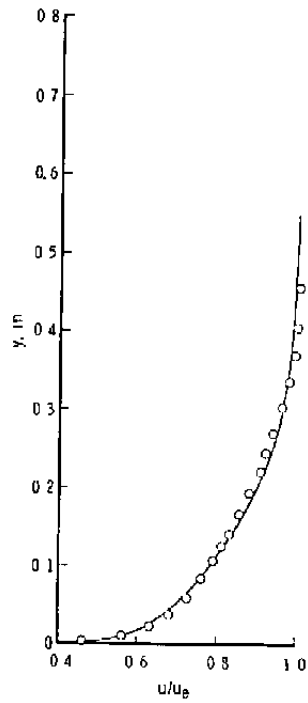
The experimentally measured velocity profiles of Simpson (Ref. 9) and Alber (Ref. 10) were fit using the above procedure; that is, for each measured profile, Eq. (20) was solved iteratively (by Newton's method) for $\bar{u}^{+}_{e}$, $\tilde{a}$, and b. These parameters are different for each velocity profile. Achieving the best fit of a given velocity profile was a trial and error process which consisted of changing the three points needed to fit the profile. Note that $\bar{u}^{+}_{e}$ is, by definition, always positive. For the separated profiles, a negative skin friction was inferred by knowing, a priori, that the measured velocity near the wall was negative. Therefore, for fitting the velocity profile, Eq. (13) was modified to be

$$S = \frac{\dfrac{\bar{u}}{\bar{u}_e}}{\left| \dfrac{\bar{u}}{\bar{u}_e} \right|} \Bigg|_{\text{at } y \text{ where } \left(-\bar{u} \ \bar{u}_e \right) \text{ is maximum.}} \qquad (21)$$

Comparisons of fitted and measured velocity profiles (separated and attached) for both experimental investigations are presented in Fig. 1. The agreement is reasonably good throughout the entire range of y. This was the case for nearly all the experimentally measured profiles considered for evaluation. For each separated profile, the best fit resulted from using the maximum negative velocity ratio as the first point from the wall.

Experimental Data of Alber et al (Ref 10)

Symbols Represent Experimental Data
Solid Line Represents Eq. (20)

a. Upstream of separation
   (Sta. -9.0)
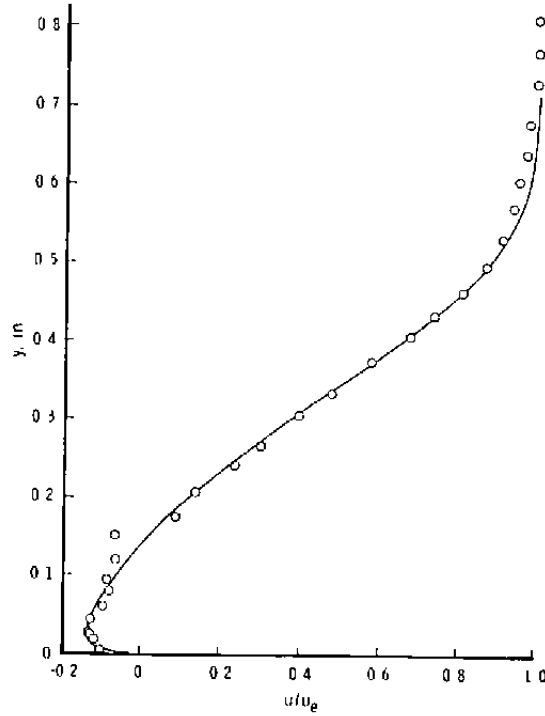
b. Within separation (Sta. 4.5)

c. Downstream of separation (Sta. 7.0)

Figure 1. Comparison of measured attached and separated
boundary-layer velocity profiles with Eq. (14).

Experimental Data of Simpson et al (Ref 9)

Symbols Represent Experimental Data
Solid Line Represents Eq (20)

d. Upstream of separation
(x=60 in.)

e. Within separation (x=139.1 in.)
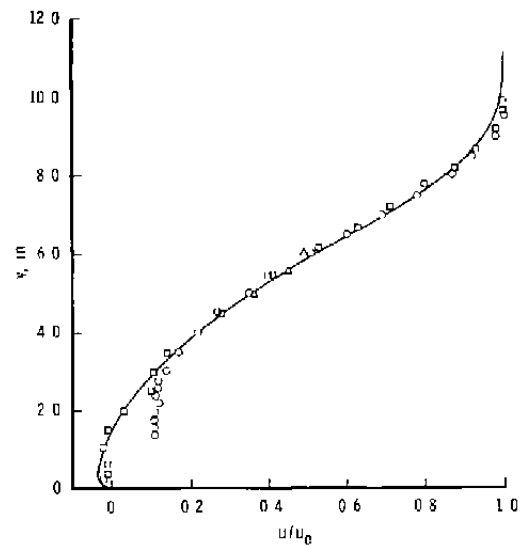
f. Within separation (x=157.1)
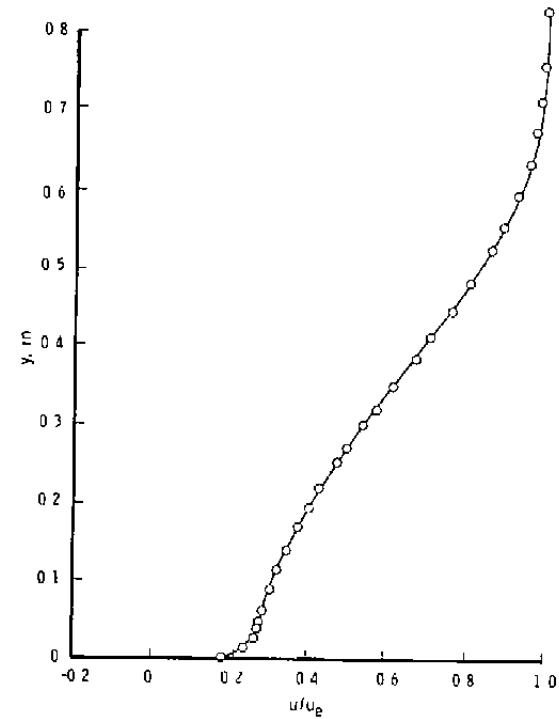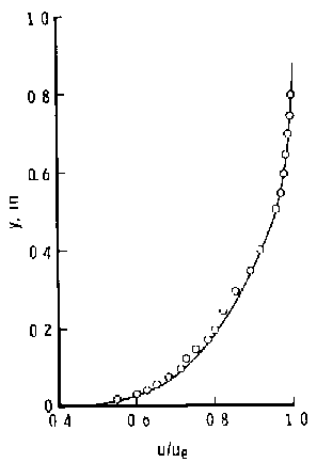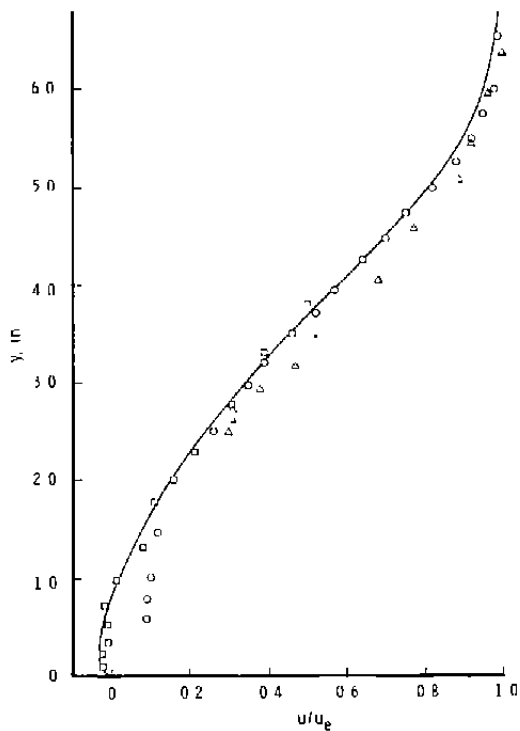
Figure 1. Concluded.

It should be noted that the measurements of Alber (Ref. 10) were in the transonic regime whereas Eq. (20) was developed for incompressible flows. However, it was reported by Lewis, Kubota, and Webb (Ref. 11) that for compressible flows (up to $M_e = 8.18$), the relation

$$(22)$$

is suitable for relating compressible variables to their incompressible counterparts. Furthermore, Whitfield (Ref. 6) shows that to a reasonable approximation

$$\frac{\bar{v}}{\bar{\theta}} \approx \frac{y}{\theta_k} \tag{23}$$

where θ_k refers to the kinematic boundary-layer momentum thickness defined by

$$\theta_k = \int_o^\infty \frac{u}{u_e} \left(1 - \frac{u}{u_e} \right) dy \tag{24}$$

Therefore, Eq. (20) is approximate for compressible flows if rewritten as

$$\bar{u}^+ = \frac{S}{0.09} \tan^{-1} (0.09 \, \bar{y}^+) + \left[\bar{u}_e^+ - \frac{S\pi}{0.18} \right] \tanh^{1/2} \left[a \left(\frac{y}{\theta_k} \right)^b \right] \tag{25}$$

where

$$\bar{y}^+ = \frac{\overline{Re}_\theta}{\bar{u}_e^+} \frac{y}{\theta_k} \tag{26}$$

and

$$\frac{\bar{u}}{\bar{u}_e} = \frac{\bar{u}^+}{\bar{u}_e^+} = \frac{u}{u_e} \tag{27}$$

and $\overline{Re}_\theta$ which appears in Eq. (26) is obtained by applying Coles' "Law of Corresponding Stations" (Ref. 12),

$$\tilde{C}_f \overline{Re}_\theta = C_f Re_\theta \tag{28}$$

in conjunction with the correlation offered by Winter and Gaudet (Ref. 13), which relates $\overline{C}_f$ to C_f by the relation $\overline{C}_f = C_f [1 + (M_e^2/5)]^{1/2}$.

3.2 SKIN FRICTION

It is of interest to compare skin frictions as determined from Eq. (20) to those reported in Refs. 9 and 10. This comparison is presented in Fig. 2, which shows skin friction versus incompressible shape factor, $\overline{H}$. Simpson (Ref. 9) measured $\overline{C}_f$ directly by flush-mounted hot film devices, whereas the skin friction reported by Alber (Ref. 10) was inferred from a least-squares fit of the measured velocity profile data to Coles' law of the wall and law of the wake (see Ref. 14). The skin friction data reported in Ref. 10 have been transformed to

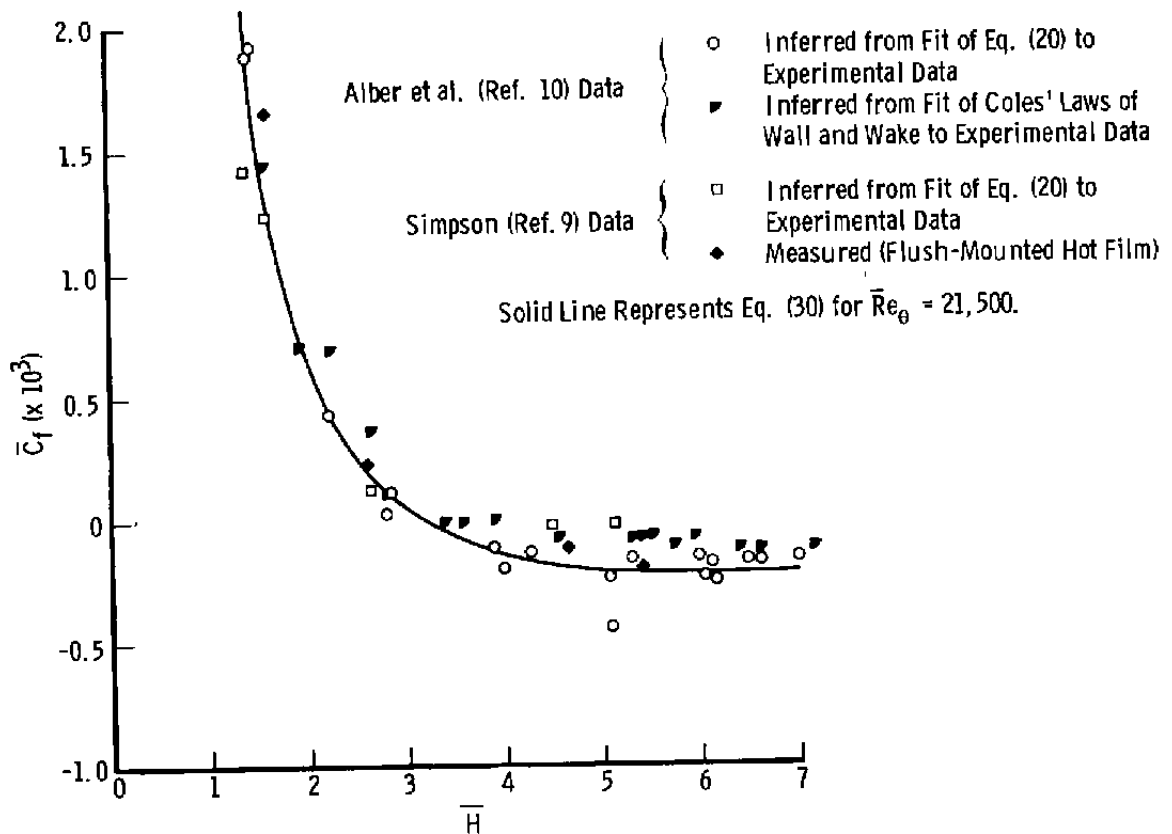Figure 2. Correlation of incompressible skin friction, $\overline{C}_f$, for separated, incompressible flow.

equivalent incompressible values as suggested by Winter and Gaudet (Ref. 13) according to the relation $\overline{C}_f = C_f [1 + (M_e^2/5)]^{1/2}$. Simpson (Ref. 9) reported that precise interpretation of his measured results was difficult downstream of intermittent separation because the

flush-mounted hot film probes used were directionally insensitive. The differences between skin frictions computed by the present method and those reported in Ref. 10 are attributed to the fact that the basic velocity profile representations are different; i.e., Eq. (20) or Coles' composite form of the law of the wall and law of the wake. The shape factor, $\overline{H}$, used in Fig. 2 was obtained by numerically integrating (using Simpson integration) the profile fit used to obtain skin friction from the simultaneous solution of Eq. (20) at three points across the layer. The shape factor, $\overline{H}$, is defined by

$$\overline{H} = \frac{\overline{\delta^*}}{\overline{\theta}} = \frac{\int_0^\infty \left(1 - \frac{\overline{u}}{\overline{u}_e}\right) dy}{\int_0^\infty \frac{\overline{u}}{\overline{u}_e}\left(1 - \frac{\overline{u}}{\overline{u}_e}\right) dy} \tag{29}$$

For the data obtained in compressible flow (Ref. 10), recourse was made to the approximation $\overline{u}/\overline{u}_e = u/u_e$, $\overline{y}/\overline{\theta} = y/\theta_k$, and thus $H_k = \overline{H}$.

The solid line in Fig. 2 represents the analytic expression derived to approximate the numerical and experimental results for $Re_\theta = 21,500$ [the average momentum thickness Reynolds number of the Alber experiment (Ref. 10)]. The expression selected was

$$\overline{C}_f = \frac{0.3 \, e^{-1.33\overline{H}}}{\left(\log_{10} \overline{Re}_\theta\right)^{1.74 + 0.31\overline{H}}} + \left(1.1 \times 10^{-4}\right)\left[\tanh\left(4 - \frac{\overline{H}}{0.875}\right) - 1\right] \tag{30}$$

The form of the second term of Eq. (30) was chosen such that for shape factors less than about 2.3, the expression degenerates into the relationship given by White (Ref. 15). Any dependence of the incompressible skin friction on Reynolds number has been assumed to be accounted for by the first term of Eq. (30) [for $\overline{H} \gtrsim 3.5$, $\overline{Re}_\theta$ has little effect on $\overline{C}_f$, according to Eq. (30)].

3.3 SHAPE FACTOR CORRELATION

The parameters a and b which appear in Eq. (14) are determined by matching the velocity distribution at two points, $\overline{y}/\overline{\theta} = 2$ and 5 (Ref. 6 discusses why $\overline{y}/\overline{\theta} = 2$ and 5 were chosen for the match points). These parameters were correlated with $\overline{H}$ (Ref. 6) by plotting $\overline{u}/\overline{u}_e$ at $\overline{y}/\overline{\theta} = 2$ and 5 versus $\overline{H}$ for numerous measured velocity profiles (Ref. 14). However, the correlations established in Ref. 6 did not include separated flow. The behavior of $\overline{u}/\overline{u}_e$ with $\overline{H}$ at $\overline{y}/\overline{\theta} = 2$ and 5 is presented in Fig. 3 for both attached and separated flow. The data were compiled in Ref. 6 from the Stanford conference (Ref. 14) and inferred from fitting the velocity profile, Eq. (14), to the measured velocity data of Simpson (Ref. 9) and Alber (Ref.

10). The dashed lines represent the correlations established in Ref. 6, and the solid lines are the present results derived by including the data inferred from the separated profiles. The correlation of $\bar{u}/\bar{u}_e$ at $\bar{y}/\theta = 2$,

$$\frac{\bar{u}}{\bar{u}_e}(2) = \frac{1}{1.95}\left[\tanh^{-1}\left(\frac{8.5 - \bar{H}}{7.5}\right) - 0.364\right] \tag{31}$$

represents the large shape factor data reasonably well (Fig. 3a) whereas the proposed variation of $\bar{u}/\bar{u}_e$ with $\bar{H}$ at $\bar{y}/\theta = 5$,

$$\frac{\bar{u}}{\bar{u}_e}(5) = 0.155 + 0.795\,\mathrm{sech}\left[0.51\,(\bar{H} - 1.95)\right] \tag{32}$$

falls below the data inferred from the Alber experiment (Fig. 3b) (Ref. 10) for $\bar{H} > 3$ but represents the data inferred from the Simpson experiment (Ref. 9) reasonably well. Both relationships approximate the Whitfield correlations (Ref. 6) for $\bar{H} < 3$. It should be noted
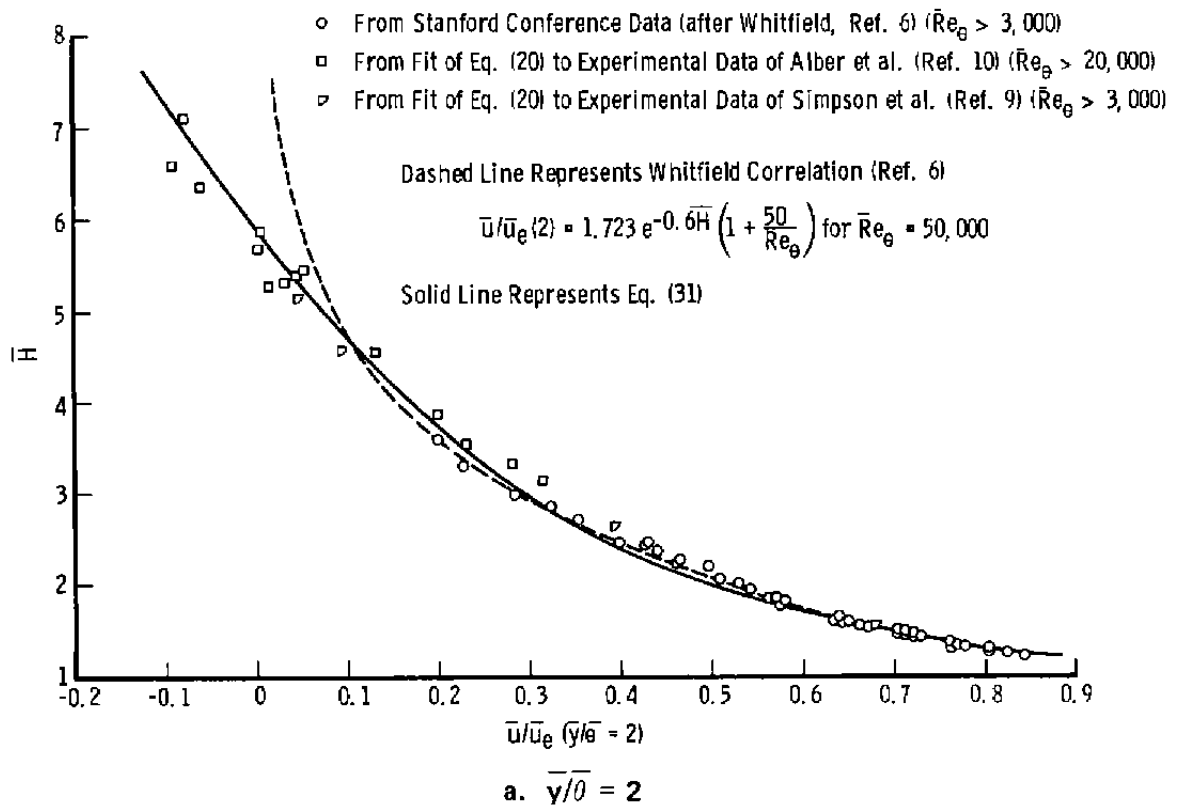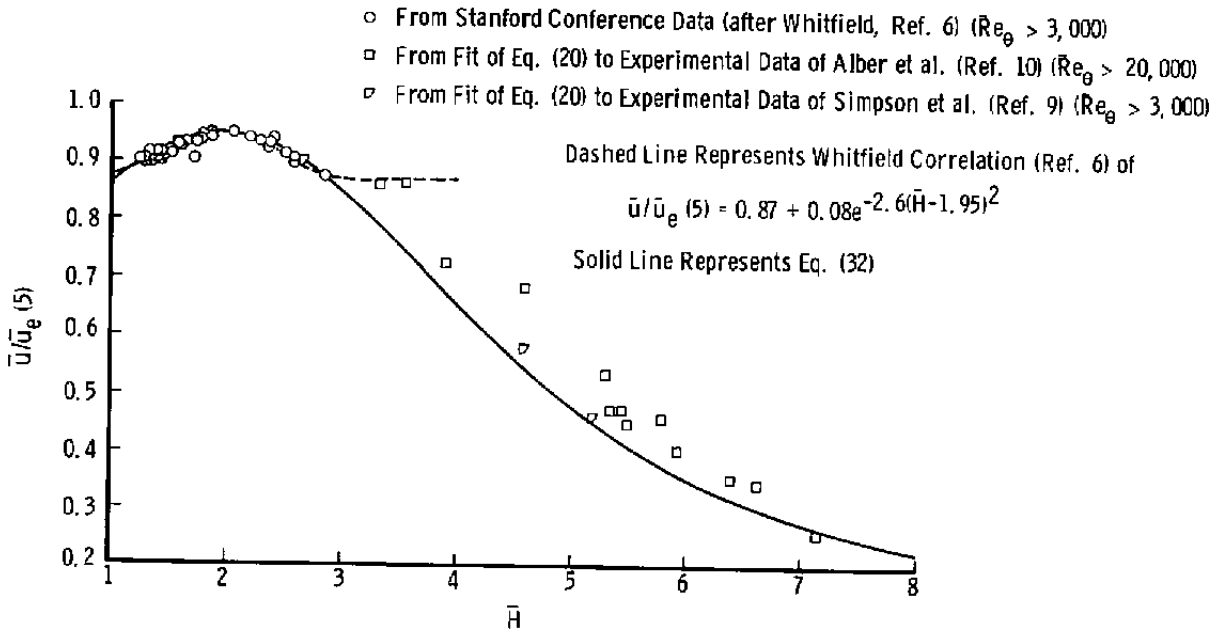

a. $\overline{y/\theta} = 2$

Figure 3. Correlation of experimental velocity profile data.

○ From Stanford Conference Data (after Whitfield, Ref. 6) ($Re_\theta > 3,000$)
□ From Fit of Eq. (20) to Experimental Data of Alber et al. (Ref. 10) ($Re_\theta > 20,000$)
▽ From Fit of Eq. (20) to Experimental Data of Simpson et al. (Ref. 9) ($Re_\theta > 3,000$)

Dashed Line Represents Whitfield Correlation (Ref. 6) of

$$\bar{u}/\bar{u}_e \ (5) = 0.87 + 0.08e^{-2.6(\bar{H}-1.95)^2}$$

Solid Line Represents Eq. (32)

b. $\overline{y/\theta} = 5$

Figure 3. Concluded.

that the $\bar{\theta}$ used in determining the velocity ratio of $\bar{y}/\bar{\theta} = 2$ and 5 was obtained by numerically integrating the fitted "raw" profile (dimensional y versus $\bar{u}/\bar{u}_e$) using the relation

$$\bar{\theta} = \int_0^{d_0} \frac{\bar{u}}{\bar{u}_e}\left(1 - \frac{\bar{u}}{\bar{u}_e}\right)dy \tag{33}$$

as opposed to using the experimentally determined momentum thickness. This was done so that the resulting correlations would be consistent with the velocity profile, Eq. (14). The relationships between compressible and incompressible variables, Eqs. (22) and (23), were used when the compressible data of Alber (Ref. 10) were correlated.

Equations (31) and (32) can be used to generate separated, incompressible, turbulent boundary-layer velocity profiles from $\overline{H}$, $\bar{u}_e^+$, and $\overline{Re}_\theta$. The procedure is outlined in Table 1.

As derived in Ref. 16, there are four integral length scales which appear in the boundary-layer momentum and mean flow kinetic energy integral equations:

$$\delta^* = \int_0^\infty \left(1 - \frac{\rho u}{\rho_e u_e}\right)dy \tag{34}$$

16

$$\theta = \int_{0}^{\infty} \frac{\rho u}{\rho_e u_e} \left(1 - \frac{u}{u_e} \right) dy \tag{35}$$

$$\theta^* = \int_{0}^{\infty} \frac{\rho u}{\rho_e u_e} \left(1 - \frac{u^2}{u_e^2} \right) dy \tag{36}$$

and

$$\delta^{**} = \int_{0}^{\infty} \frac{u}{u_e} \left(1 - \frac{\rho}{\rho_e} \right) dy \tag{37}$$

In addition, the following shape factors were defined in Ref. 16:

$$H_{\delta^*} = \frac{\delta^*}{\theta} \tag{38}$$

$$H_{\theta^*} = \frac{\theta^*}{\theta} \tag{39}$$

$$H_{\delta^{**}} = \frac{\delta^{**}}{\theta} \tag{40}$$

these shape factors were also correlated as a function of $\overline{H}$ and boundary-layer edge Mach number, M_e. For the present work, attention will be restricted to establishing a relationship between H_{θ^*} and $\overline{H}$ for incompressible flow, $M_e \approx 0$. As a consequence, the correlations derived in Ref. 16 for $H_{\delta^*} = H_{\delta^*}(\overline{H}, M_e)$ and $H_{\delta^{**}} = H_{\delta^{**}}(\overline{H}, M_e)$ remain unchanged because for $M_e \approx 0$, H_{δ^*} is approximately equal to $\overline{H}$ and $H_{\delta^{**}}$ is approximately equal to 0.

The velocity profile, Eq. (14), was used to carry out the numerical integrations (using Simpson's integration) necessary to establish the correlation between H_{θ^*} and $\overline{H}$. Because $\overline{C}_f = \overline{C}_f(\overline{H}, \overline{Re}_\theta)$, Eq. (30), the velocity profile is only a function of $\overline{H}$ and $\overline{Re}_\theta$. As pointed out by Whitfield (Ref. 16), the influence of $\overline{Re}_\theta$ on the velocity profile is small compared to that of $\overline{H}$. The results presented are for a representative turbulent momentum thickness Reynolds number, $\overline{Re}_\theta = 50,000$.

Figure 4 presents the numerical results for $H_{\theta^*} = H_{\theta^*}(\overline{H})$ as open symbols. The analytic expression

$$H_{\theta^*} = 1.48061 + 3.83781\, e^{-2\overline{H}} + 0.33 - \frac{1}{8.5484} \tan^{-1} \left[\frac{10^{7-\overline{H}} - 1}{1.23} \right]$$

$$-\left(0.33 - \frac{\pi}{17.1} \right) \tanh^{1/2} \left[\left(1.2874 \times 10^{-6} \right) \left(10^{7-\overline{H}} \right)^{1.45761} \right] \tag{41}$$

was chosen to represent the numerical results.

Table 1. Summary of Procedure for Computation of Separated Turbulent Boundary-Layer Velocity Distributions

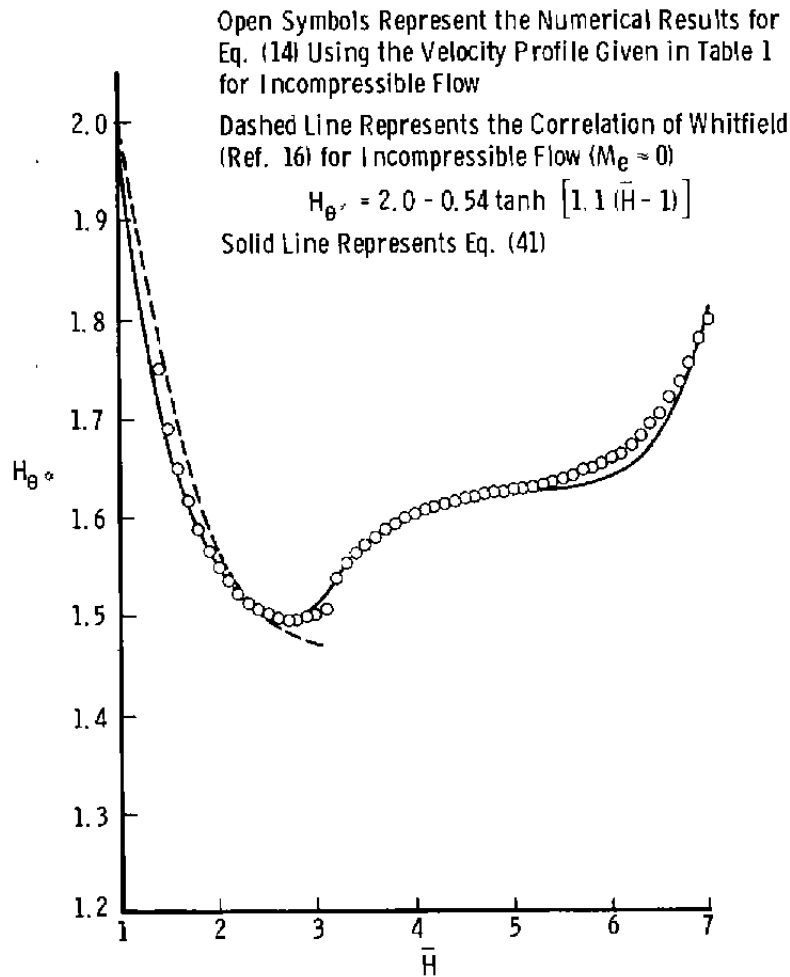| Step	Requirement	Eq. No.	Comment
1	$\bar{\Pi}$, $\bar{u}_e^+$, $\bar{Re}_\theta$ must be given	—	$\bar{u}_e^- = \left(2/|\tilde{C}_f|\right)^{1/2}$
2	Compute $S = \dfrac{\tilde{C}_f}{|\tilde{C}_f|}$	(13)	$\bar{C}_f = \bar{C}_f\left(\bar{Re}_\theta, \bar{\Pi}\right)$, Eq.(30)
3	Compute $\dfrac{\bar{u}}{\bar{u}_e}(2) = \dfrac{1}{1.95}\left[\tanh^{-1}\left(\dfrac{8.5 - \bar{\Pi}}{7.5}\right) - 0.364\right]$	(31)	$\dfrac{\bar{u}}{\bar{u}_e}\left(\dfrac{\bar{y}}{\bar{\theta}}\right)$ at $\dfrac{\bar{y}}{\bar{\theta}} = 2$
4	Compute $\dfrac{\bar{u}}{\bar{u}_e}(5) = 0.155 + 0.795\, \text{sech}\left[0.51(\bar{\Pi} - 1.95)\right]$	(32)	$\dfrac{\bar{u}}{\bar{u}_e}\left(\dfrac{\bar{y}}{\bar{\theta}}\right)$ at $\dfrac{\bar{y}}{\bar{\theta}} = 5$ $\text{sech}(z) = \dfrac{2}{e^z + e^{-z}}$
5	Compute $g(2) = \dfrac{\dfrac{\bar{u}}{\bar{u}_e}(2) - \dfrac{S}{0.09\bar{u}_e^+}\tan^{-1}\left(\dfrac{0.18\bar{Re}_\theta}{\bar{u}_e^+}\right)}{1 - \dfrac{S\pi}{0.18\bar{u}_e^+}}$	(10), (11)	$g\left(\dfrac{\bar{y}}{\bar{\theta}}\right)$ at $\dfrac{\bar{y}}{\bar{\theta}} = 2$
6	Compute $g(5) = \dfrac{\dfrac{\bar{u}}{\bar{u}_e}(5) - \dfrac{S}{0.09\bar{u}_e^+}\tan^{-1}\left(\dfrac{0.45\bar{Re}_\theta}{\bar{u}_e^+}\right)}{1 - \dfrac{S\pi}{0.18\bar{u}_e^+}}$	(10), (11)	$g\left(\dfrac{\bar{y}}{\bar{\theta}}\right)$ at $\dfrac{\bar{y}}{\bar{\theta}} = 5$
7	Compute $b = \dfrac{\ell n\left\{\dfrac{\tanh^{-1}\left[g^2(2)\right]}{\tanh^{-1}\left[g^2(5)\right]}\right\}}{\ell n\left(\dfrac{2}{5}\right)}$	(11)	$\tanh^{-1}(z) = \dfrac{1}{2}\ell n\left(\dfrac{1+z}{1-z}\right)$
8	Compute $a = \dfrac{\tanh^{-1}\left[g^2(2)\right]}{2^b}$	(11)	$\tanh(z) = \dfrac{e^{2z} - 1}{e^{2z} + 1}$
9	$\bar{u}^+ = \dfrac{S}{0.09}\tan^{-1}\left(0.09\bar{y}^+\right) + \left(\bar{u}_e^- - \dfrac{S\pi}{0.18}\right)\tanh^{1/2}\left[a\left(\dfrac{\bar{y}}{\bar{\theta}}\right)^b\right]$	(14)	$\dfrac{\bar{u}}{\bar{u}_e} = \dfrac{u}{u_e} = \dfrac{\bar{u}^+}{\bar{u}_e^+}$ $\bar{y}^+ = \dfrac{\bar{Re}_\theta}{\bar{u}_e^+} \cdot \dfrac{\bar{y}}{\bar{\theta}}$

Open Symbols Represent the Numerical Results for
Eq. (14) Using the Velocity Profile Given in Table 1
for Incompressible Flow

Dashed Line Represents the Correlation of Whitfield
(Ref. 16) for Incompressible Flow ($M_e \approx 0$)

$$H_{\theta'} = 2.0 - 0.54 \tanh \left[1.1 (\bar{H} - 1) \right]$$

Solid Line Represents Eq. (41)

Figure 4. Correlation of $H_{\theta}*$ for adiabatic,
incompressible flow.

4.0 CONCLUDING REMARKS

An analytical expression that reasonably describes the velocity distribution in a separated, turbulent boundary layer has been developed. The expression is an extension of the form derived by Whitfield (Ref. 6) for attached flows on smooth, impermeable, adiabatic walls. The analytical expression was fit to available experimentally measured, separated velocity profiles to establish velocity correlations for u/u_e at $\bar{y}/\bar{v} = 2$ and 5 and to establish a local skin friction correlation in the form $\overline{C_f} = \overline{C_f}(\bar{H}, \overline{Re}_v)$, which allows $\overline{C_f}$ to become negative. These correlations and the analytical velocity profile expression were used to obtain a reversed flow boundary-layer shape factor correlation. The analytical velocity profile expression depends on local values of skin friction, shape factor, and Reynolds

number based on momentum thickness, and describes attached or separated flow over the entire y domain $(0 \leq y < \infty)$.

Because of the relatively small amount of experimental data which were available, the relations developed cannot yet be considered universally applicable to all flow situations. The correlations should be improved as more experimental data become available.

REFERENCES

1. Assassa, G. M. and Papailiou, K. D. "An Integral Method for Calculating Turbulent Boundary Layer with Separation." *Journal of Fluids Engineering*, Vol. 101, March 1979, pp. 110-116.

2. Cebeci, Tuncer. "Separated Flows and Their Representation by Boundary-Layer Equations." ONR-CR215-234-2, September 1976.

3. Kuhn, Gary D. and Nielsen, Jack N. "Prediction of Turbulent Separated Boundary Layers in Subsonic and Transonic Flows." AIAA Paper No. 73-663, July 1973.

4. Carter, J. E. "A New Boundary-Layer Interaction Technique for Separated Flow." AIAA Paper No. 79-1450, July 1979.

5. Moses, H. L., Jones, R. R. III, O'Brien, W. F., and Peterson, R. S., Jr. "Simultaneous Solution of the Boundary Layer and Freestream with Separated Flow." *AIAA Journal*, Vol. 16, No. 1, January 1978, pp. 61-66.

6. Whitfield, D. L. "Analytical Description of the Complete Two-Dimensional Turbulent Boundary-Layer Velocity Profile." AEDC-TR-77-79 (ADA045033), September 1977; AFSC also AIAA Paper No. 78-1158, July 1978.

7. Whitfield, D. L. "Analytical, Numerical, and Experimental Results on Turbulent SAF/OIS Boundary Layers." AEDC-TR-76-62 (ADA027588), July 1976.

8. Clauser, F. H. "Turbulent Boundary Layers in Adverse Pressure Gradients." *Journal of the Aeronautical Sciences*, Vol. 21, No. 2, February 1954, pp. 91-108.

9. Simpson, R. L., Strickland, J. H., and Barr, P. W. "Features of a Separating Turbulent Boundary Layer in the Vicinity of Separation." *Journal of Fluid Mechanics*, Vol. 79, Part 3, 9 March 1977, pp. 553-594.

10. Alber, I. E., Bacon, J. W., Masson, B. S., and Collins, D. J. "An Experimental Investigation of Turbulent Transonic Viscous-Inviscid Interactions." *AIAA Journal*, Vol. 11, No. 5, May 1973, pp. 620-627.

11. Lewis, J. E., Kubota, T., and Webb, W. H. "Transformation Theory for the Adiabatic Compressible Turbulent Boundary Layer with Pressure Gradient." *AIAA Journal*, Vol. 8, No. 9, September 1970, pp. 1644-1650.

12. Coles, D. E. "The Turbulent Boundary Layer in a Compressible Fluid." Rand R-403-PR(AD285651), Rand Corporation, Santa Monica, California, September 1962.

13. Winter, K. G. and Gaudet, L. "Turbulent Boundary-Layer Studies at High Reynolds Numbers at Mach Numbers Between 0.2 and 2.8." Aeronautical Research Council, London, R&M No. 3712 (ARC33345), December 1970.

14. Coles, D. E. and Hirst, E. A., Editors. *Proceedings, Computation of Turbulent Boundary Layers - 1968 AFOSR-IFP-Stanford Conference: Vol. II, Compiled Data.* Thermosciences Division, Department of Mechanical Engineering, Stanford University, California, 1968.

15. White, F. M. *Viscous Fluid Flow.* McGraw-Hill Book Company, Inc., New York, 1974.

16. Whitfield, D. L. "Integral Solution of Compressible Turbulent Boundary Layers Using Improved Velocity Profiles." AEDC-TR-78-42 (ADA062946), December 1978.

NOMENCLATURE

a   Parameter in Eqs. (11), (12), (14), (18), and (19)

$\tilde{a}$ Defined by Eq. (19)

b   Parameter in Eqs. (11), (12), (14), (18), and (19)

C_f Local skin friction coefficient, $2\tau_w/\varrho_e u_e^2$

g   Function defined by Eq. (11)

$\overline{H}$ Incompressible shape factor, defined by Eq. (29)

H_{δ^*} Shape factor based on δ^*, defined by Eq. (38)

$H_{\delta^{**}}$	Shape factor based on δ^{**}, defined by Eq. (40)
H_{θ^*}	Shape factor based on θ^*, defined by Eq. (39)
M	Mach number
Re	Local unit Reynolds number, u_e/ν_e
Re_θ	Local momentum thickness Reynolds number, $u_e\theta/\nu_e$
S	Parameter defined by Eq. (13)
u	Mean velocity in the axial direction
u^+	Boundary-layer velocity coordinate, u/u_τ
u_i^+	Inner solution for u^+
u_o^+	Outer solution for u^+
u_τ	Friction velocity, $(|C_f|/2)^{1/2}\,u_e$
x	Coordinate along body surface
y	Coordinate normal to body surface
y^+	Boundary-layer y coordinate, $u_\tau y/\nu$
δ^*	Boundary-layer displacement thickness, defined by Eq. (34)
δ^{**}	Boundary-layer density thickness, defined by Eq. (37)
θ	Boundary-layer momentum thickness, defined by Eq. (35)
$\bar{\theta}$	Equivalent incompressible momentum thickness, defined by Eq. (33)
θ^*	Boundary-layer energy thickness, defined by Eq. (36)
θ_k	Boundary-layer kinematic momentum thickness, defined by Eq. (24)
ν	Kinematic viscosity
ϱ	Density
τ	Total shear stress

SUBSCRIPTS

e   Boundary-layer edge value

i   Inner region of a boundary layer

o   Outer region of a boundary layer

w   Wall value

∞ Infinity or free-stream value

SUPERCRIPTS

—   Denotes low-speed or incompressible value

$'$ Denotes fluctuating quantity

SPECIAL NOTATION

$<\ >$ Indicates time-averaged quantity, e.g., $<uv> = \lim_{t \to \infty} \frac{1}{2t} \int_{-t}^{t} (uv)\, dt$